Impacts of Air-Sea Interaction on Tropical Cyclone Track and Intensity

Liguang Wu[1,2], Bin Wang[3], and Scott A. Braun[2]

[1]Goddard Earth and Technology Center, University of Maryland at Baltimore County, Baltimore, Maryland.

[2]Laboratory for Atmospheres, NASA Goddard Space Flight Center, Greenbelt, Maryland.

[3]Department of Meteorology, School of Ocean and Earth Science and Technology University of Hawaii at Manoa, Honolulu, Hawaii.

Submitted to Mon. Wea. Rev.

May 2004

*Corresponding author address: Dr. Liguang Wu, NASA/GSFC, Code 912, Greenbelt, MD 20771

E-mail: liguang@agnes.gsfc.nasa.gov

ABSTRACT

The influence of hurricane-ocean coupling on intensity and track of tropical cyclones (TCs) is investigated through idealized numerical experiments using a coupled hurricane-ocean model. The focus is placed on how air-sea interaction affects TC tracks and intensity. It is found that the symmetric sea surface temperature (SST) cooling is primarily responsible for the TC weakening in the coupled experiments because the induced asymmetric circulation associated with the asymmetric SST anomalies is weak and shallow. The track difference between the coupled and fixed SST experiments is generally small because of the competing processes. One is associated with the modified TC asymmetries. The asymmetric SST anomalies weaken the surface fluxes in the rear and enhance the fluxes in the front. As a result, the enhanced diabatic heating is located on the southern side for a westward-moving TC, tending to shift the TC southward. The symmetric SST anomalies weakens the TC intensity and thus the axisymmetrization process, leading to more prominent TC asymmetries. The other is associated with the weakening of the beta drift resulting from the weakening of the TC outer strength. In the coupled experiment, the weakening of the beta drift leads to a more northward shift. By adjusting the vortex outer strength of the initial vortices, the beta drift can vary while the effect of air-sea interaction changes little. Two types of track differences simulated in the previous numerical studies are obtained.

1 Introduction

A tropical cyclone (TC) develops and maintains itself by drawing its primary energy from the underlying ocean surface. It can form only over waters of 26°C or higher and its intensity is very sensitive to the sea surface temperature (SST) (e.g., Tuleya and Kurihara 1982, Emanuel 1986). Emanuel (1988) developed a theory that treats a tropical storm as a Carnot heat engine and suggested that the TC maximum potential intensity (MPI) is primarily determined by the underlying SST. At the same time, the surface wind stress associated with a TC can generate strong turbulent mixing, deepening of the ocean mixed layer (ML) and entrainment of cooler water to the surface that can lead to significant SST decrease. Observations indicate that the SST cooling caused by TCs ranges from 1°C to 6°C (Price 1981).

The feedback of the resulting cooling on TC intensity has been investigated using coupled hurricane-ocean models. Early experiments were performed with axisymmetric TC models that were coupled with upper ML ocean models (Elsberry et al. 1976; Chang and Anthes 1979; Sutyrin and Khain 1979). Because of the markedly rightward bias of the ocean response with respect to the TC track, three-dimensional coupled models were used (Bender et al. 1993; Falkovich et al. 1995; Chan et al. 2001). These simulations have indicated in general that the storm-induced cooling of the sea surface has a significant impact on the storm intensity. Previous studies argued that model TCs subjected to air-sea interaction are weaker than the corresponding ones without air-sea interaction. Although more realistic simulations can

be achieved with a three-dimensional coupled model, Emanuel (1999) was able to successfully simulate the evolution of storm intensity using a two-dimensional (axially symmetric) hurricane model coupled with a one-dimensional ocean model. This suggests that the symmetric component of the storm-induced SST anomaly field may play a decisive role in reducing the ultimate storm intensity. Note that the amplitude of the TC-induced asymmetric SST anomaly is larger than that of the symmetric counterpart. Whether this minor symmetric SST anomalies can be fully responsible for the reduction of final intensity is not clear.

While the previous studies generally agree with each other regarding the effect of air-sea interaction on TC intensity, they disagree concerning the impacts on TC motion. Khain and Ginis (1991) found that westward-moving (eastward-moving) TCs in coupled experiments were displaced farther to the south (north) than in the corresponding experiments without air-sea interaction. They attributed these track differences to asymmetric precipitation patterns which were shifted azimuthally because of air-sea interaction. On the other hand, Bender et al. (1993), by coupling the NOAA Geophysical Fluid Dynamics Laboratory (GFDL) TC prediction model with an eight-layer ocean model, found that the westward tracks in the coupled model gradually turned more to the north of the one in the fixed SST experiments and that the largest impact on the TC track occurred with slow moving storms. Bender et al. (1993) suggested that this track deviation is related to a systematic decrease in the azimuthally averaged tangential flow of the TC vortex. What causes these

contradictory results calls for further investigation.

The main objective of this study is to further our understanding of the mechanisms responsible for the changes in TC intensity and track. The ocean response to TC forcing comprises a weaker axially symmetric component of SST cooling but a stronger asymmetric SST component relative to the TC center. The different roles of the two components are conceivable, but the way by which the two components affect TC intensity and motion and their relative roles have not been directly addressed. The emphasis of this study is on how the symmetric and asymmetric responses of the ocean temperature affect TC intensity and track. The present study will specifically address this issue through idealized numerical experiments by use of a hydrostatic primitive equation hurricane model coupled with an ocean model with intermediate complexity. The model details and the experimental design are described in section 2. The ocean and TC responses to hurricane-ocean interaction are presented in sections 3 and 4, respectively. The main conclusions are summarized in section 5.

2 The coupled hurricane-ocean model and experimental design

a. Hurricane model

The hurricane model designed by Wang (1998) is adopted in this study. The model consists of 201×201 grid points with a uniform spacing of 25 km and 16 ver-

tical layers with relatively high resolution near the lower and upper boundaries. The details of the model and its capability to simulate the motion and evolution of baroclinic TCs in the presence of diabatic heating has been documented by Wu (1999) and Wu and Wang (1999). The primary model physics includes large-scale condensation calculated explicitly with the method used by Leslie et al. (1985), subgrid-scale cumulus convection parameterized with Kuo's (1974) scheme, a Newtonian cooling as used in the TC model by Rotunno and Emanuel (1987), and surface fluxes of momentum, sensible and latent heat calculated by the bulk aerodynamic method, in which the exchange coefficients are determined from the formula given by Kondo (1975) for neutral conditions and modified to be Richardson number-dependent following Louis (1979).

b. Ocean model

The ocean response to the forcing of a moving hurricane may be conveniently divided into the forced and relaxation stages (Gill 1984). The forced stage response, lasting typically half a day or a storm residence time, is a primarily local response, which includes ML currents of 1 $m\ s^{-1}$ and substantial cooling of the ML by the vertical mixing (Price 1981; Sanford et al. 1982; Black 1983; Shay et al. 1992). Following a hurricane passage, the relaxation stage response is an inherently nonlocal baroclinic response to the wind stress curl, lasting typically 5-10 days. The energy is spreading through internal waves (Geisler 1970; Gill 1984) that penetrate into

the thermocline (Shay and Elsberry 1987; Brink 1989), eventually leaving behind a baroclinic geostrophic current along the storm track. In order to simulate these ocean responses, the ocean model should describe the ML physics and thermocline and upper ocean dynamics.

A two and one half layer ocean model developed by Wang et al. (1995) is used in this study. Since the response is primarily baroclinic, the ocean upper boundary is a rigid lid so that the barotropic response is removed. The model includes two active upper layers: a ML and a middle thermocline layer. Below the thermocline layer is a motionless deep layer ($z < -h$) in which the temperature (T_r) is assumed to be constant. In the ML ($0 > z > -h_1$), the temperature (T_1) and velocity are independent of depth, and in the thermocline layer ($-h_1 > z > -h$), the temperature decreases linearly from T_1 to T_r.

Since the ocean model was originally developed for study of ocean phenomena on the interannual time scale, the model physics are modified to better simulate the ocean response to the forcing of a moving hurricane. First, following Bender et al. (1993), the Kraus-Turner scheme (Kraus and Turner 1967) to parameterize the vertical turbulent mixing (entrainment) is replaced by the Deardorff's scheme (Deardorff 1983) to include the important shear instability (Ginis 1995). According to Deardorff (1983), a singularity occurs in the Kraus-Turner scheme when the velocity shear is significant.

Second, the TC-ocean interaction is through the surface turbulent fluxes of mo-

mentum, sensible and latent heat. The energetics of the mixed layer has been studied extensively for the last two decades. Although no consensus exists on the amount of turbulent energy radiated from the mixed layer, some theoretical and laboratory analysis suggest that the bulk of the energy fed into the mixed layer is trapped by the transition layer and is eventually dissipated by wave breaking (Fernando 1991). Ginis (1995) suggested that this condition is probably appropriate for the ocean areas that experience the most intense TCs. In this model, it is assumed that the downward heat flux decreases exponentially in the mixed layer and the turbulent momentum and heat fluxes are not allowed to penetrate below the ML base in the modified ocean model.

Third, as mentioned by Wang et al. (1995), parameterization of the temperature of entrained water is another key to closure of the mixed layer equations. Consider a thin entrainment layer existing just below the ML base. This entrainment layer is a thin region of vigorous small-scale mixing, within which the turbulent flux drops sharply from a finite value to zero. If its thickness is Δh_e, we assume that the vertical temperature gradient in the entrainment layer is proportional to the mean vertical temperature gradient in the thermocline layer, that is

$$T_1 - T_e = k\Delta h_e \frac{T_1 - T_r}{h - h_1}, \tag{1}$$

where k is the proportional constant. In Wang et al.(1995) model, $k = 1$, implying that the vertical temperature gradient in the entrainment layer is equal to the mean vertical temperature gradient in the thermocline layer. In the response of the ocean

to the TC forcing, as shown by Shay et al. (1992), the temperature gradient between the ML and the top of the thermocline can be much larger than the mean vertical temperature gradient in the thermocline. For this reason, in the following coupled experiments, we assume $k = 3$, based on the results of Shay et al. (1992).

In this study, the ocean is initially assumed to be horizontally homogeneous and quiescent. The water temperature in the deep resting layer is set to 10^oC. The entrainment layer depth is 5 m, which is identical to that used by Wang et al.(1995). The initial ML depth and temperature are also two important parameters. Sensitivity tests show that the magnitude of the cooling in this layer increases with decreasing initial depth or increasing initial SST. Moreover, the magnitude of the ML cooling also increases with increasing depth or temperature gradient associated with the thin entrainment layer. However, the cooling patterns are generally similar. For this reason, the depth of the mixed layer is initially set to 35 m in all coupled experiments. The ocean model has the same grid spacing and domain size as the hurricane model. The SST and wind stress are passed between the hurricane and ocean models every 3 minutes. Periodic lateral boundary conditions are used in the hurricane and ocean models.

c. Experimental design

The effects of air-sea coupling and the associated symmetric and asymmetric forcing of the corresponding SST variations on TC behavior are examined through

three sets of numerical experiments (Table 1). The first set of numerical experiments (E1) are run on an f-plane with a horizontally uniform easterly ambient flow -4 ms^{-1}. The second set of numerical experiments (E2) are designed on a beta plane in a resting environment, in which the vortex movement arises from the beta drift. The third set of numerical experiments (E3) are a combination of E1 and E2, including the influences of uniform easterly flow and the beta effect.

For each group, four experiments are conducted: Fixed SST, coupled, symmetric SST forcing, and asymmetric SST forcing. In the fixed SST experiment, the air-sea coupling is excluded and the SSTs are fixed and horizontally uniform (29.5°C for E1 and 28.5°C for E2 and E3). The second experiment is run with full air-sea coupling. Air-sea interaction affects TC intensity primarily through the induced SST anomaly since uncoupled numerical experiments conducted with the time-dependent SST forcing generated in the coupled experiments indicate that the resulting TC track and intensity are nearly identical to the corresponding coupled experiments. The SST anomalies produced in the coupled experiments are saved each hour and are therefore decomposed into their symmetric and asymmetric components with respect to the TC center. The symmetric SST component can directly affect the intensity of the TC's symmetric circulation while the asymmetric component affects TC through the interaction between the mean TC circulation and the induced asymmetric circulation. Because the ways by which the two components influence TC intensity and track are different, two more uncoupled experiments are run using the symmetric

and asymmetric SST anomalies respectively. For convenience, these experiments are called symmetric and asymmetric SST forcing experiments in this paper.

All experiments begin with an identical, initially symmetric baroclinic vortex. The intensity of the initial vortex decreases with height, but without anticyclonic circulation atop. The maximum wind (v_m) of 25 ms^{-1} at r_m=100 km is at the lowest model level. The horizontal wind profile ($v(r)$) is generated following

$$v(r) = v_m(\frac{r}{r_m})exp\frac{1}{b}[1 - (\frac{r}{r_m})^b], \quad (2)$$

where r and b are the radius from the TC center and the shape parameter. b is set to 0.5 in sets E1, E2 and E3. The change in this parameter primarily affects the outer strength of the initial vortex, which can further affect the behavior of the beta drift. In order to examine the influence of air-sea interaction on the beta drift, three additional experiments conducted in this study are the same as E2 except the shape parameter, which is 0.3 for B1, 1.0 for B2 and 1.2 for B3.

3 Ocean response in the coupled model

In this section we focus on the coupled experiment of E2C since the patterns of the ocean response to TC forcing are similar. Figure 1 shows the time series of the maximum current speeds in the ML and thermocline layer (Fig. 1a) and the minimum ML temperature (Fig. 1b). The ML current increases quickly while the minimum temperature decreases rapidly during the first 24 h. Both reach a quasi-

steady state after 24 h while the thermocline current continues to accelerate until 72 h. The maximum mixed layer cooling of 3.5°C occurs at 33 h. This magnitude is consistent with ocean observations. Black (1983) found that storm moving faster (slower) than 3 ms^{-1} can produce 1-3°C (3-5°C) cooling (The TC speed or the beta drift in E2C is 2-4ms^{-1}). When the SST reaches its minimum value, the ML current is about 1.1 ms^{-1}. Thereafter the current intensifies slightly and attains its maximum of 1.2 ms^{-1} at 56 h. The magnitude of the resulting ML currents also compares favorably with observations (e.g., Shay et al. 1992) and numerical simulations with other sophisticated coupled models (e.g., Bender et al. 1993).

Figure 2 shows the spatial distributions of the ocean responses at 96 h in E2C. Negative SST anomalies cover a large area and form a cold wake along the TC track (Fig. 2a). The cooling has a pronounced rightward bias with respect to the TC track and the maximum cooling is located behind the TC center. The pattern of the ML cooling is consistent with the rightward-biased ML deepening (Fig. 2b). The strong entrainment rate which is parameterized as a function of wind stress, velocity shear at the base of the mixed layer, and convective overturning due to the surface buoyancy fluxes is primarily confined to the vicinity of the TC center (Fig. 2c), suggesting that the dynamics of the ocean inertia-gravity waves excited by moving TCs also contribute to the ML deepening in the wake of the TC (Gill 1984). The feature of the response depends strongly on whether the TC speed exceeds the long gravity wave speed or not. In this case, the phase velocity of long gravity waves is about 1.2 ms^{-1}

for the first baroclinic mode, and the translation speed of the TC is greater than the gravity wave speed in this coupled model. As a result, the characteristic feature of the baroclinic response was an oscillating narrow wake behind the storm.

The region of the maximum ML deepening occurs well behind the TC center on the right hand side of the TC track. The maximum deepening reaches 63 m at 44 h and decreases to about 45 m at 96 h. This is comparable with the observational analysis of Hurricane Gilbert (1988) by Shay et al. (1992). They found that storm passage increased the ML depth from prestorm values of 30-35 m to approximately 60 m on the right hand side of the track. The pattern of ML deepening is also similar to that simulated with the GFDL coupled model for Hurricane Norbert (Bender et al. 1993). The model ML currents are presented in Fig. 2e. In the front of the TC, the cyclonically rotating wind stress generates the ML currents with significant divergence and the current pattern becomes significantly asymmetric behind the TC. The thermocline depth displays negative anomalies behind the TC center without significant biases with respect to the track (Fig. 2d). The weak positive anomalies outside the negative anomalies are an indication of the horizontal dispersion of inertia-gravity waves after the TC passing while the thermocline current (Bender et al. 1993), which is primarily driven by the depth gradient, shows a rightward bias (Fig. 2f). Compared with the ML currents, the resulting thermocline currents are small.

In summary, the major features of the simulated ocean response in the current coupled hurricane-ocean model, i.e., the amplitudes and spatial patterns of the ML

cooling and deepening, the thermocline depth anomalies, and the induced ocean currents in the mixed and thermocline layers, are all in good agreement with observations and previous numerical simulations. Therefore, the current ocean model is capable of realistically simulating the effect of air-sea interaction on TCs.

4 Influence of air-sea interaction on TCs

a. Intensity change

Figure 3 shows the time series of TC intensity in terms of the maximum wind speed and the minimum central pressure. The influences of air-sea interaction on TC intensity in E1, E2 and E3 can be seen by comparing with the corresponding fixed-SST experiments (Fig. 3). In agreement with previous numerical studies (e.g., Chang and Anthes 1979; Khain and Ginis 1991; Bender et al. 1993), the present simulations confirm that air-sea coupling reduces TC intensity as a result of mixed layer cooling. The simulated TCs maintain a relatively steady state in intensity after 36 hours. The effect of air-sea coupling can occur as early as 12 h when the TCs are undergoing rapid intensification. The reduction in TC intensity is nearly constant after the intensities of the simulated storms reach a steady state. In absence of air-sea coupling (E1F), the TC reaches a maximum wind of 60.1 ms^{-1} and a central pressure of 917 mb. While with coupling (E1C), the maximum wind is reduced by about 12 ms^{-1} and the central surface pressure decreases by 32 mb. In E2, the

coupling (E2C) leads to differences of 14 ms^{-1} and 24 mb in the maximum wind speed and the minimum central pressure, respectively. When the beta effect and environmental flow are combined (E3), the time of maximum wind of is somewhat delayed. Due to air-sea interaction, the maximum wind is reduced by 10 ms^{-1} and the central pressure by 18 mb.

Figure 4 shows the decomposition of the SST anomaly field shown in Fig. 2a. The symmetric SST anomaly extends over a large area with an average magnitude of 1.5°C in the inner core region. The asymmetric SST pattern shows a cold wake of negative anomalies behind the center and weak positive anomalies in front of the center. Although the magnitudes of the negative anomalies are generally larger, the maximum cooling is located well behind the center. As shown in Fig. 3, the TC intensities in the symmetric and asymmetric SST forcing experiments are nearly identical to those in the coupled and fixed-SST experiments, respectively, except for small fluctuations. This result suggests that the intensity differences between the coupled and the fixed-SST experiments are primarily caused by the symmetric component of the induced SST drop while the asymmetric component of the resulting SST anomalies only plays a minor role in the intensity change resulting from air-sea coupling.

In principle, the asymmetric SST field can affect TC intensity through the the resulting inner-core TC asymmetries and surface fluxes. In order to examine the asymmetries associated with the asymmetric SST forcing, the total asymmetric winds

in the fixed-SST experiments are compared with those in the asymmetric forcing experiments. The differences of the asymmetric winds between these two experiments are considered to be the result of the asymmetric SST forcing. Figure 5 shows an example in E2. It can be seen that the asymmetric winds resulting from the asymmetric SST anomalies are quite weak. The winds induced by the asymmetric SST forcing (Fig. 5b) are mainly confined to a small region associated with the significant SST anomalies. Moreover, the resulting asymmetric winds are confined primarily to the lower model levels (figure not shown).

Using the same hurricane model, Wu and Braun (2004) investigated the role of hurricane inner-core asymmetries that result from large-scale environmental influences. They found that the inner-core asymmetries weaken TC intensity through the eddy momentum fluxes associated with the resulting asymmetries. The eddy fluxes tend to decelerate tangential and radial winds in the inflow and outflow layers in the vicinity of the eyewall. The corresponding changes in the symmetric circulation tend to counteract the deceleration effect. As a result, the net effect is a moderate weakening of the mean tangential and radial winds. The reduced radial wind can be viewed as an anomalous secondary radial circulation with inflow in the upper troposphere and outflow in the lower troposphere. However, the hurricane flow asymmetries that arise from the asymmetric SST anomalies are weak and shallow, so they play an insignificant role in TC intensity change.

b. TC tracks

The tracks between the coupled and fixed SST experiments are shown in Fig. 6. For the experiments in E1, E2, and E3, the track differences are similar to those of the westward-moving TCs simulated by Khain and Ginis (1991). By 96 h, the track differences in experiments E1, E2, and E3 are 29, 100, and 40 km, respectively. The track differences can be associated with the shift in the rainfall pattern. Wu and Wang (2001) suggested that wavenumber-one diabatic heating with respect to the TC center can directly affect TC motion by generating a positive potential vorticity tendency. The asymmetry of diabatic heating can be displayed in the rainfall rate field since the diabatic heating is dominated by the latent heat release.

Figure 7 shows the total rainfall rates at 24, 60 and 96 h for the fixed experiment of E1 (E1F) (Fig. 7a) and the corresponding asymmetric (E1A) (Fig. 7b) and symmetric (Fig. 7c) forcing (E1S) experiments. The mechanisms responsible for the generation of the rainfall asymmetry have been discussed in previous studies. Superposition of a uniform environmental flow on the TC circulation in the planetary boundary layer can provide surface flux asymmetries that enhance the diabatic heating in the region with relatively high winds. Shapiro (1983) suggested that asymmetries in surface friction caused by vortex translation tend to produce a wavenumber-one asymmetry in convergence, with the maximum eyewall convergence ahead and slightly to the right of the storm motion vector for slow moving TCs. The enhanced rainfall rates on the right and front sides of the eyewall (relative to the

westward motion) in Fig. 7 indicates that these mechanisms likely operate in the E1 experiments.

Although the rainfall rates appear qualitatively similar, the time-dependent symmetric and asymmetric SST anomalies produce two distinct changes in the rainfall asymmetries. First, as shown in Fig. 7b, the positive SST anomaly in the asymmetric forcing experiment increases the rainfall rate ahead of the TC center after 24 h when the ML temperature changes are well developed (Fig. 1b). Compared with Fig. 7a, rainfall maxima on the western and southwestern sides of the eyewall are intensified. Second, the warmer mean SST than that in the coupled and symmetric forcing experiments leads to more intense TC circulation in the asymmetric forcing and fixed-SST experiments. The asymmetries appear less in the fixed-SST and asymmetric forcing experiments because the stronger storms axisymmetrizes the asymmetries more effectively than the weaker storms. This is consistent with the fact that intense hurricanes tend to be rather symmetric (Willoughby et al. 1984).

The shift of the rainfall pattern is conceptually similar to the mechanism discussed by Khain and Ginis (1991), but while they attribute the shift to the SST cooling behind the center, in this case the shift appears related more to the smaller warming ahead of the center. If the asymmetric cooling was the cause of the shift, one should expect a reduction of precipitation relative to that in Fig. 7a rather than an increase in Fig. 7b.

The TC track differences showing in Fig. 8 are consistent with the asymmetries

of the rainfall pattern. In the fixed SST experiment, the TC persistently moves northwestward before 72 h (Fig. 8). The shift of the rainfall asymmetry from the northwest to the west side between 60 and 96 h (Fig. 7a) causes the TC to move westward. Although it is primarily steered by the easterly environmental flow, in response to this shift of the rainfall pattern, it starts to take a southward shift at 48 h (Fig. 8). In the symmetric SST experiment, the strongest rainfall is persistent on the northern side and the TC moves northwestward. Based upon this analysis, we conclude that the symmetric and asymmetric SST anomalies associated with the air-sea interaction modify the asymmetry of the rainfall rate or diabatic heating with respect to the TC center and thus impact TC tracks. The asymmetric SST forcing intensifies the rainfall rate on the front left side while the symmetric forcing weakens the TC intensity and concurrently the axisymmetrization process. In E1, these two effects are opposite so that the resulting track difference between the coupled and fixed-SST experiments is relatively small (Fig. 6a).

Figures 9 and 10 show the rainfall rates of the coupled and fixed-SST experiments for E2 and E3. For the fixed SST experiment of E2 (Fig. 9a), the TC moves northwestward (Fig. 7b) and the rainfall at 24 h intensifies primarily ahead of the TC center. As time progresses, the beta gyres develop and intensify and gradually lead to a shift in the precipitation pattern. In addition to the boundary layer mechanism discussed above, the beta gyres and their associated southeasterly vertical shear can also affect the asymmetries of the precipitation. Peng et al. (1999) suggested that

the asymmetric flow of the beta gyres increases the inward radial wind in the southeastern quadrant and increases the tangential wind in the northeastern part of the TC. As a result, the largest surface fluxes are expected to be located in the eastern and southeastern part. Also, in the presence of vertical wind shear, convection tends to be enhanced on the downshear-left side (Frank and Richie 1999, 2001; Reasor et al. 2000). At 48 h and 72 h, the primary rainfall rate maximum in the fixed-SST experiment of E2 shifts to the eastern side in agreement with the expected impacts of the beta gyres. For the fixed-SST experiment of E3 (Fig. 10a), the rainfall pattern is similar to that shown in Fig. 7a, suggesting the dominant role of the boundary layer mechanism in the asymmetries of the precipitation.

In the presence of air-sea coupling (Figs. 9b and 10b), the rainfall patterns exhibit more prominent wavenumber-one asymmetries. With the maxima of the rainfall rates generally occurring in the southern part of the TCs, we hypothesize that the favorable location is associated with the asymmetric SST anomalies resulting from air-sea coupling. If we consider the cyclonic rotation of air parcels as they rise, the enhanced (suppressed) rainfall rates are related to the positive (negative) SST anomalies ahead of (behind) the TC center. These persistent rainfall asymmetries tend to shift the TC tracks southward in the coupled experiments of E2 and E3 (Figs. 7b,c).

Bender et al. (1993) suggested that in experiments with air-sea interaction a systematic weakening of the mean tangential flow at all radii tends to occur. This weakening alters the orientation of the beta gyres and thus affects the beta drift

(Fiorino and Elsberry 1989). The resulting secondary steering flow associated with the beta gyres in the coupled experiments rotates anticyclonically relative to that in the fixed-SST experiments (Wang et al. 1997). Therefore the weakening of the mean tangential wind tends to shift TCs northward. The resulting track deviations from the fixed-SST experiments are therefore a result of the competing effects of asymmetric SST anomalies and changes in the beta drift associated with air-sea coupling. For this reason, the net track differences between the coupled and fixed-SST experiments are generally small.

The influence of the beta drift and its association with the vortex size can be investigated by modifying the initial vortex profile by adjusting the shape parameter (b). In E1, E2 and E3, $b = 0.5$. When b is made smaller (larger) than 0.5, the outer portion of the vortex is strengthened (weakened). Since the vortex intensity does not change, the influence of air-sea interaction on the SST cooling also changes little. When the outer part of the vortex is stronger ($b = 0.3$, Fig. 5c), the vortex shifts more southward whereas when the vortex strength is weaker ($b = 1.0$ and 1.2, Figs. 5e and 5f), the vortex shifts more northward. This result is consistent with Bender et al. (1993).

5 Conclusions

The impacts of air-sea interaction on TC intensity and track are investigated through idealized numerical experiments using a hydrostatic primitive coupled

hurricane-ocean model. Compared with observations and previous numerical simulations, the coupled model can reasonably produce the major features of the ocean responses to moving TC forcing, including ML deepening, SST cooling and the ML and thermocline layer currents. The induced SST cooling consists of the symmetric SST anomalies that extend over a wide area and the asymmetric SST anomalies that show a cold wake behind the TC center and weak warming in front of the center.

In order to clarify the contradictory results in previous studies, the present study specifically focuses on the different effects of the symmetric and asymmetric SST anomalies induced by the air-sea interaction on TC intensity and track. Three sets of idealized numerical experiments that begin with an initially symmetric baroclinic vortex are designed. In the each set, four numerical experiments are conducted with fixed SST (uncoupled), air-sea coupling, symmetric SST forcing, and asymmetric SST forcing. For the latter two, the time-dependent SST forcing is deduced from the hourly output of the corresponding coupled experiments.

The present study confirms that air-sea coupling reduces TC intensity as a result of ML cooling. Although the negative SST anomalies associated with the asymmetric component are generally larger in magnitude than those associated with the symmetric component, the influence of the asymmetric anomalies is insignificant while the resulting symmetric cooling plays a decisive role in the weakening of TC intensity. The reason is that the asymmetric SST forcing affect TC intensity only through the resulting TC circulation asymmetries and surface fluxes. The asymmet-

ric winds induced by the asymmetric SST forcing are mainly confined to the lower boundary and are much weaker than the asymmetric winds induced by large-scale environmental influences such as uniform flows and the beta effect. Thus this result agrees with Emanuel's finding that the evolution of storm intensity can be successfully simulated by including only the symmetric SST cooling caused by air-sea coupling.

The track difference between the fixed SST and coupled experiments results from the processes associated with the symmetric and asymmetric SST components resulting from air-sea coupling. The symmetric and asymmetric SST anomalies modify the asymmetry of the diabatic heating with respect to the TC center, thus affecting TC motion. The asymmetric SST forcing intensify the rainfall rates on the front left side (relative to TC motion) while the symmetric SST forcing weakens the TC intensity and thus weakens the axisymmetrization process. In addition, in the presence of the beta effect, the weakening of the outer portion n the weakening of TC intensity of the mean vortex alters the orientation of the beta gyres and leads to more northward beta drift. In the f-plane case (E1), the asymmetric SST anomalies intensify the rainfall rate on the front left side while the weakened axisymmetrization leads to more prominent rainfall on the northern side. In the presence of the beta effect (E2 and E3), the enhanced TC asymmetries tend to shift TCs southward while the reduced beta drift tends to shift TCs northward in the coupled experiments. Due to the opposite effects, the resulting track difference between the fixed-SST and coupled experiments is generally small.

The different effects of air-sea interaction on TC tracks in the previous studies (Khain and Ginis 1991; Bender et al. 1993) likely result from the TC wind profiles. As demonstrated in this study, by adjusting the vortex outer strength, both types of track deviations can be achieved. When the vortex strength is relatively weak (strong), a TC in the coupled model moves to the north (south) of the TC in the corresponding fixed SST experiments.

REFERENCES

Bender, M. A., I. Ginis and Y. Kurihara 1993: Numerical simulations of hurricane-ocean interaction with a high resolution coupled model. *J. Geophys. Res.*, **98 (D12)**, 23,245-23,263.

Black, P. G., 1983: Ocean temperature changes induced by tropical cyclones. Ph. D dissertation, Pennsylvania State University, 278pp.

Brink, K. H., 1989: Observations of the response of the thermocline currents to a hurricane. *J. Phys. Oceanogr.*, **19**, 1017-1022.

Chan, J. C.-L., Y. Duan, and L. K. Shay, 2001: Tropical cyclone intensity changes from a simple ocean-atmosphere coupled model. *J. Atmos. Sci.*, **58**, 154-172.

Chang, S. W., and R. A. Anthes, 1979: The mutual response of the tropical cyclone and the ocean. *J. Phys. Oceanogr.*, **9**, 128-135.

Deardorff, J. W., 1983: A multi-limit layer entrainment formulation. *J. Phys. Oceanogr.*, **13**, 988-1002.

Elsberry, R. L., T. S. Fraim, and R. N. Trapnell, Jr. 1976: Mixed layer model of the oceanic thermal response to hurricanes. *J. Geophys. Res.*, **81**, 1153-1163.

Emanuel, K. A., 1999: Thermodynamic control of hurricane intensity. *Nature*, **401**, 665-669

Emanuel, K. A., 1988: The Maximum intensity of hurricanes. *J. Atmos. Sci.*, **45**, 1143-1155.

Emanuel, K. A., 1986: An air-sea interaction theory for tropical cyclones: I: Staedy-state maintenance. *J. Atmos. Sci.*, **43**, 585-604.

Falkovich, A. I., A. P. Khain, and I. Ginis, 1995: Motion and evolution of binary tropical cyclones in a coupled atmosphere-ocean numerical model. *Mon. Wea. Rev.*, **123**, 1345-1363.

Fernando, H. J., 1991: Turbulent mixing in stratified fluids. *Annu. Rev. Fluid Mech*, **23**, 455-493.

Fiorino, M. J., and R. L. Elsberry, 1989: Some aspects of vortex structure related to tropical cyclone motion. *J. Atmos. Sci.*, **46**, 975-990.

Frank, W. M., and E. A. Ritchie, 1999: Effects on environmental flow upon tropical cyclone structure. *Mon. Wea. Rev.*, **127**, 2044-2061.

—, and —, 2001: Effects of vertical wind shear on the intensity and structure of numerically simulated hurricanes. *Mon. Wea. Rev.*, **129**, 2249-2269.

Geisler, J. E., 1970: Linear theory of the response of a two layer ocean to a moving hurricane. *Geophys. Fluid Dyn.*, **1**, 249-272.

Gill, A. E., 1984: On the behavior of inertial waves in the wakes of storm. *J. Phys. Oceanogr.*, **14**, 1129-1151.

Ginis, I., 1995: Ocean response to tropical cyclones. Chap.5 in Global Perspectives on tropical cyclones. WMO/TD-No. 693, 218-256.

Khain, A. P., and I. Ginis. 1991: The mutual response of a moving tropical cyclone and the ocean. *Beitr. Phys. Atmos.*, **64**, 125-141.

Kondo, J., 1975: Air-sea bulk transfer coefficients in diabatic conditions. *Bound.-Layer Meteor.*, **9**, 91-112.

Kraus, E. B., and J. S. Turner, 1967: A one-dimensional model of the seasonal thermocline. Part II: The general theory and its consequences. *Tellus*, **19**, 98-105.

Kuo, H. L., 1974: Further studies of the parameterization of the influence of cumulus convection on large-scale flow. *J. Atmos. Sci.*, **31**, 1232-1240.

Leslie, L. M., G. A. Mills, L. W. Logan, D. J. Gauntlett, G. A. Kelly, M. J. Manton, J. L. McGregor, and J. M. Sardie, 1985: A high resolution primitive equations NWP model for operations and research, *Aust. Meteor. Mag.*, **33**, 11-35.

Loise, J. F., 1979: A parametric model of vertical eddy fluxes in the atmosphere. *Bound.-Layer Meteror.*, **17**, 746-756.

Peng, M. S., B.-F. Jeng, and R. T. Williams, 1999: A numerical study on tropical cyclone intensification. Part I: Beta effect and mean flow

effect. , *J. Atmos. Sci.*, **56**, 1404-1423.

Persing, J., M. T. Montgomery, and R. E. Tuleya, 2002: Environmental interactions in the GFDL hurricane model of Hurricane Opal. *Mon. Wea. Rev.*, **130**, 298-317.

Price, J. F., 1981: Upper ocean response to a hurricane. *J. Phys. Oceanogr.*, **11**, 153-175.

Reasor, P. D., M. T. Montgomery, F. D. Marks Jr., and J. F. Gamache, 2000: Low-wavenumber structure and evolution of the hurricane inner core observed by airborne dual-Doppler radar. *Mon. Wea. Rev.*, **128**, 1653-1680.

Rotunno, R., and K, A. Emanuel, 1987: An air-sea interaction theory for tropical cyclones. Part II: Evolutionary study using a nonhydrostatic axisymmetric numerical model. *J. Atmos. Sci.*, **44**, 542-561.

Sanford, T. B., P. G. Black, J. R. Haustein, J. W. Feeney, G. Z. Forristall, and J. F. Price, 1987: Ocean response to a hurricane. Part I: Observations. *J. Phys. Oceanogr.*, **17**, 2065-2083.

Shapiro, L. J., 1983: Asymmetric boundary layer flow under a translating hurricane. *J. Atmos. Sci.*, **40**, 1984-1998.

Shay, L. K., R. L. Elsberry, 1987: Near-inertial ocean current response to hurricane Frederic. *J. Phys. Oceanogr.*, **17**, 1249-1269.

Shay, L. K., P. G. Black, A. J. Mariano, J. D. Hawkins, and R. L. Elsberry, 1992: Upper ocean response to Hurricane Galbert. *J. Geophys. Res.*, **97**, 20227-20248.

Tuleya, R. E., and Y. Kurihara, 1982: A note on the sea surface temperature sensitivity of a numerical model of tropical storm genesis. *Mon. Wea. Rev.*, **110**, 2063-2069.

Willoughby, H. E., F. D. Marks Jr., and R. J. Feinberg, 1984: Stationary and moving convective bands in hurricanes. *J. Atmos. Sci.*, **41**, 3189-3211.

Wang, B., X. Li, and L. Wu, 1997: Hurricane beta drift direction in horizontally sheared flows. *J. Atmos. Sci.*, **54**, 1462-1471.

Wang, B., T. Li, and P. Chang, 1995: An intermediate model of the tropical Pacific ocean. *J. Phys. Oceanogr.*, **25**, 1599-1616.

Wang, Y., 1998: On the bogusing of tripical cyclones in numerical models: The influence of vertical structure. *Meteor. Atmos. Phys.*, **65**, 153-170.

Wu, L., and S. A. Braun, 2004: Effects of environmentally induced asymmetries on hurricane intensity: A numerical study. submitted to *J. Atmos. Sci.*.

Wu, L., 1999: Study of tropical cyclone motion with a coupled hurricane-

ocean model. Ph. D dissertation, Department of Meteorology, University of Hawaii, 212pp.

Wu, L., and B. Wang, 2000: A potential vorticity tendency diagnostic approach for tropical cyclone motion. *Mon. Wea. Rev.*, **128**, 1899-1911.

Wu, L., and B. Wang, 2001: Effects of convective heating on movement and vertical coupling of tropical cyclones: A numerical study. cyclones. *J. Atmos. Sci.*, **58**, 3639-3649.

Table 1: Summary of the numerical Experiments

	Fixed SST	Coupled	Sym. SST	Asy. SST
f-plane, -4 ms^{-1}	E1F	E1C	E1S	E1A
β-plane, 0 ms^{-1}	E2F	E2C	E2S	E2A
β-plane, -4 ms^{-1}	E3F	E3C	E3S	E3A

List of Figures

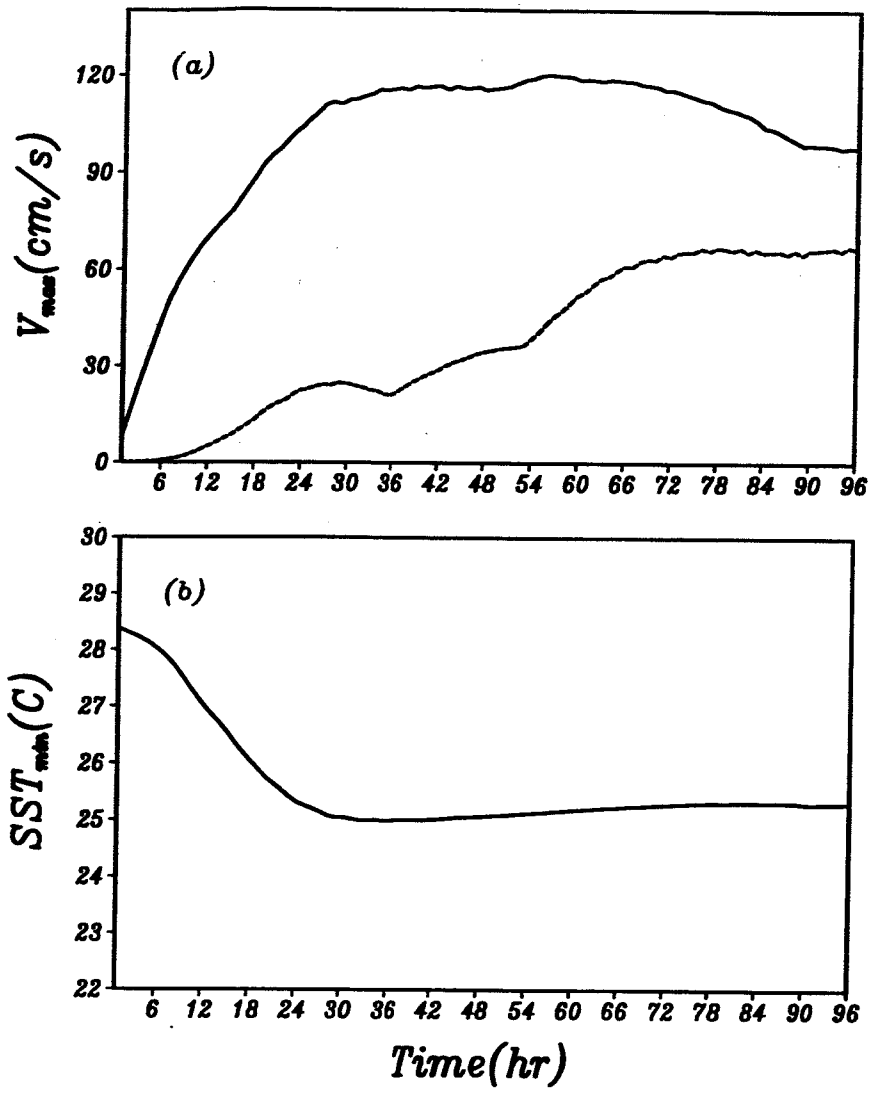

Figure 1: Time series of the maximum ocean responses: (a) currents (cms^{-1})in the mixed (solid) and thermocline (dashed) layers and (b) sea surface temperature.

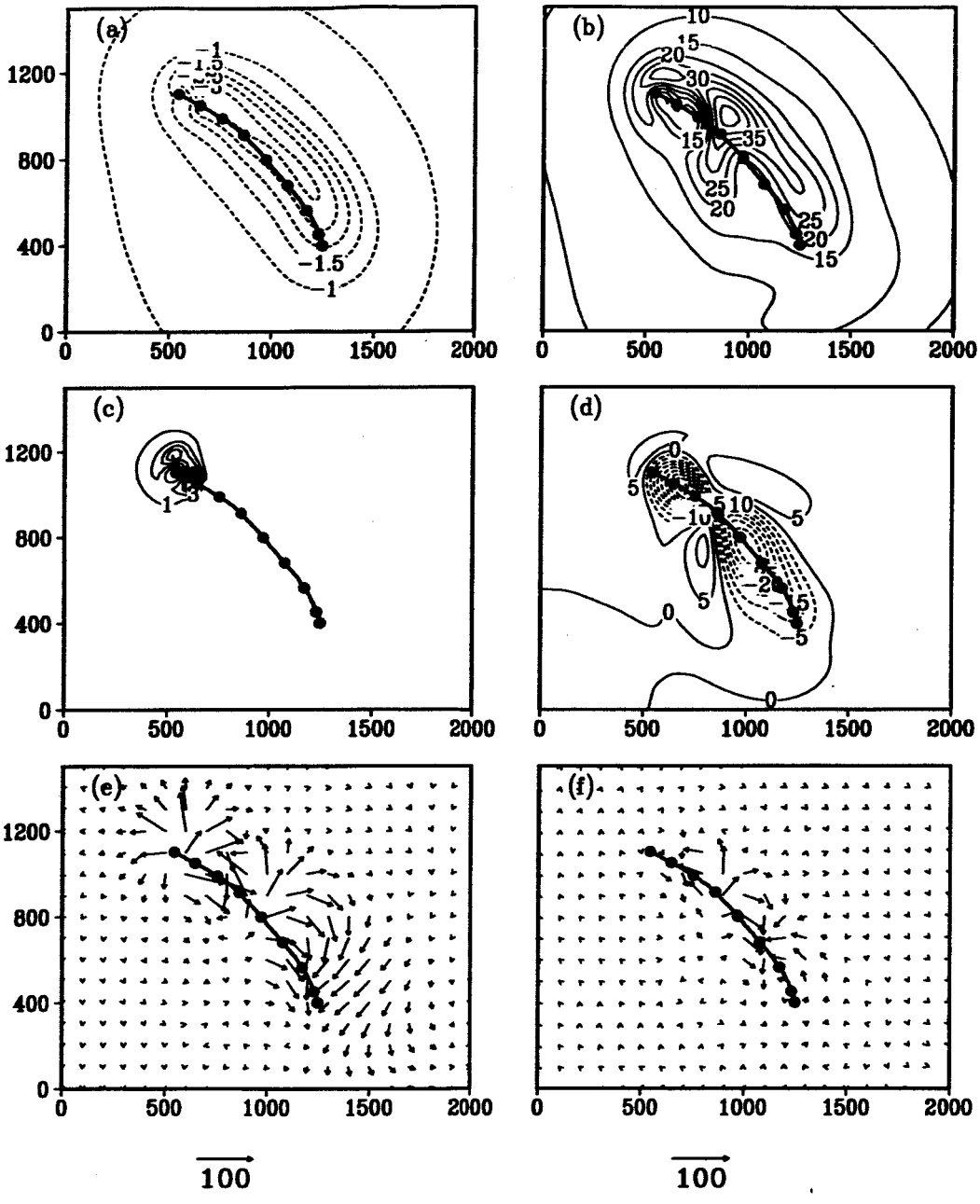

Figure 2: 96 h ocean responses in the coupled experiment of E2 (E2C) : (a) sea surface temperature anomaly (^oC); (b) mixed layer depth anomaly (m); (c) entrainment rate (cms^{-1}); (d) thermocline depth anomaly (m); (e) currents in the mixed layer (cms^{-1}), and (f) currents in the thermocline layer (cms^{-1}).

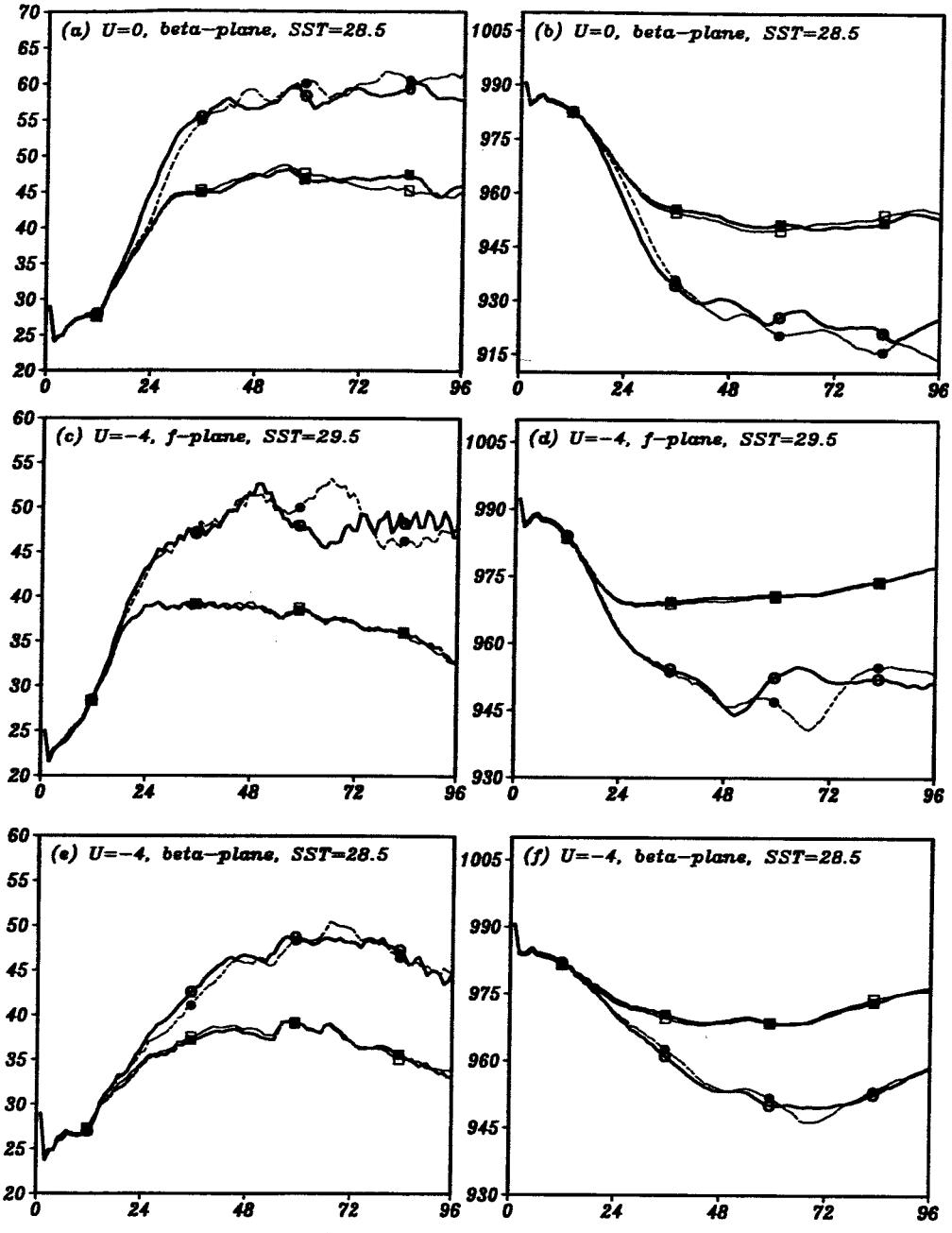

Figure 3: Time series of the maximum wind speed (left) and minimum central pressure (right) in experiments E2 (a and b), E1 (c and d) and E3 (d and f). The open and solid circles denote the fixed and asymmetric SST experiments while the open and solid squares indicate the coupled and symmetric SST experiments.

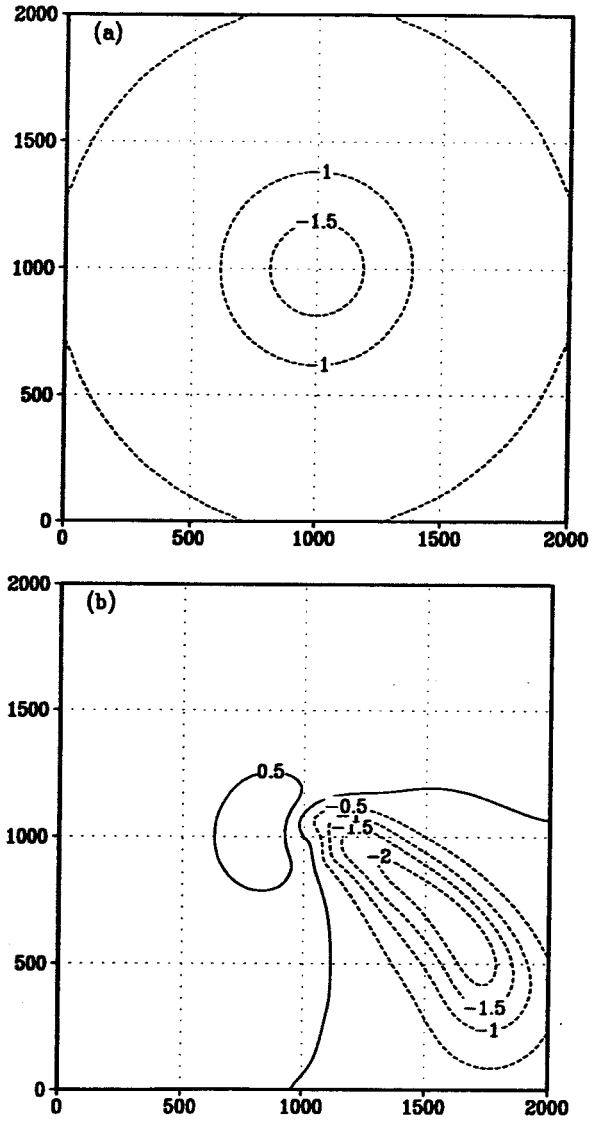

Figure 4: Decomposition of the SST anomalies at 96 h resulting from hurricane-ocean interaction in the coupled experiment of E2 (E2C): (a) the symmetric SST component and (b) the asymmetric SST component (^oC). Contour intervals are 0.5^oC.

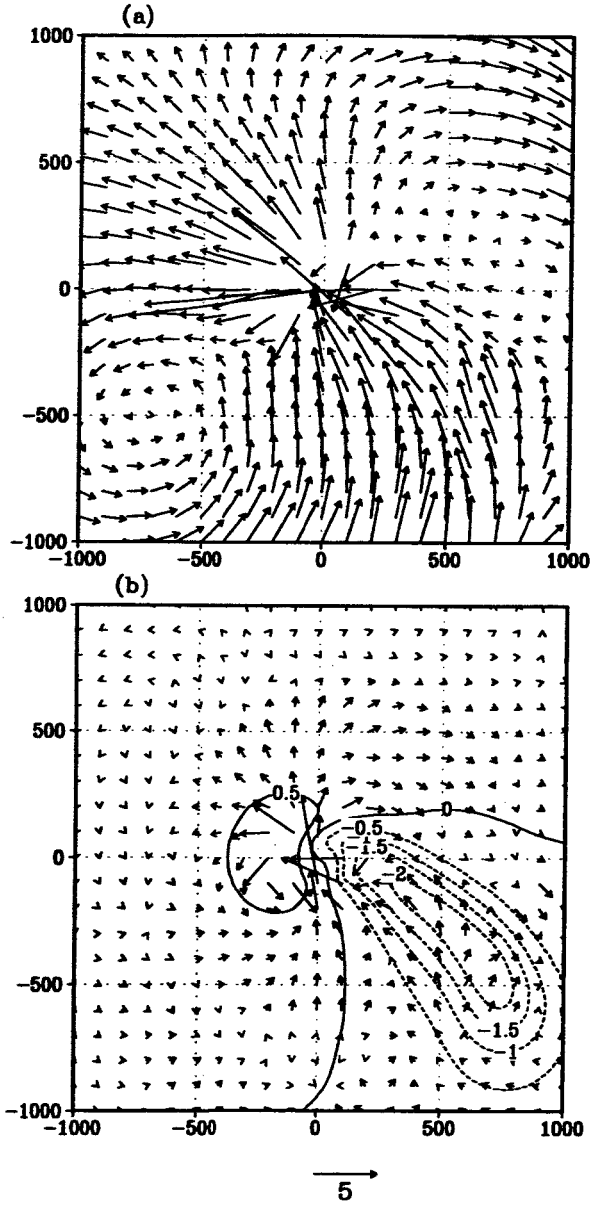

Figure 5: (a) The lowest-level (about 990 mb) asymmetric wind field in the fixed SST experiment of E2 (E2F) and (b) the wind difference between the asymmetric forcing (E2A) and fixed SST (E2F) experiments of E2 at 96 h. The asymmetric component of the SST anomalies is superposed at an interval of 0.5^oC. The TC is located at the domain center.

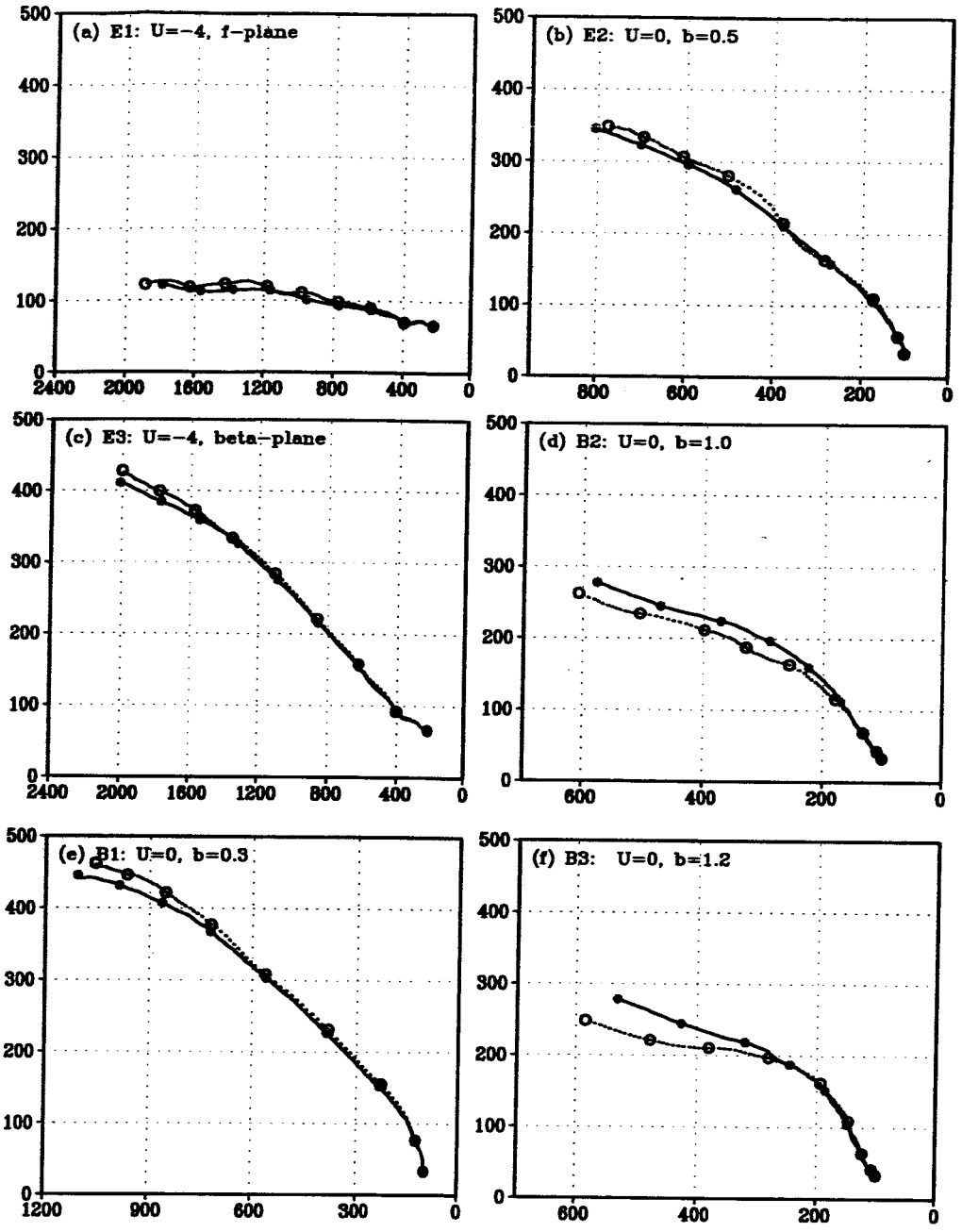

Figure 6: TC tracks in the fixed SST (dashed) and coupled (solid) experiments for (a) E1, (b) E2, (c) E3, (d) B2, (e) B1, and (f) B3. Every 12-h center locations are indicated with circles.

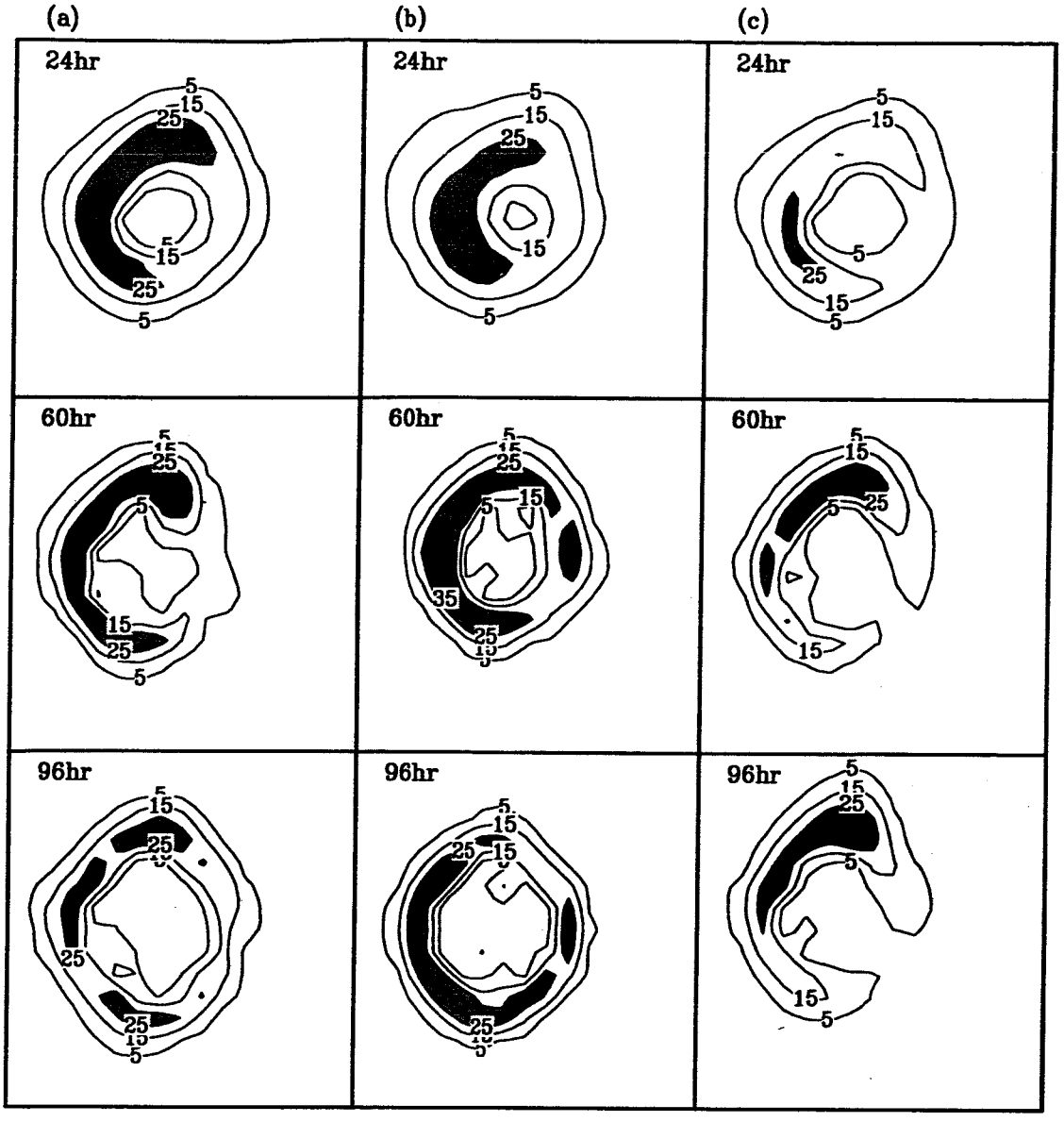

Figure 7: Rainfall rate (mmh^{-1}) in (a) the fixed SST, (b) asymmetric forcing, and (c) symmetric forcing experiments of E1.

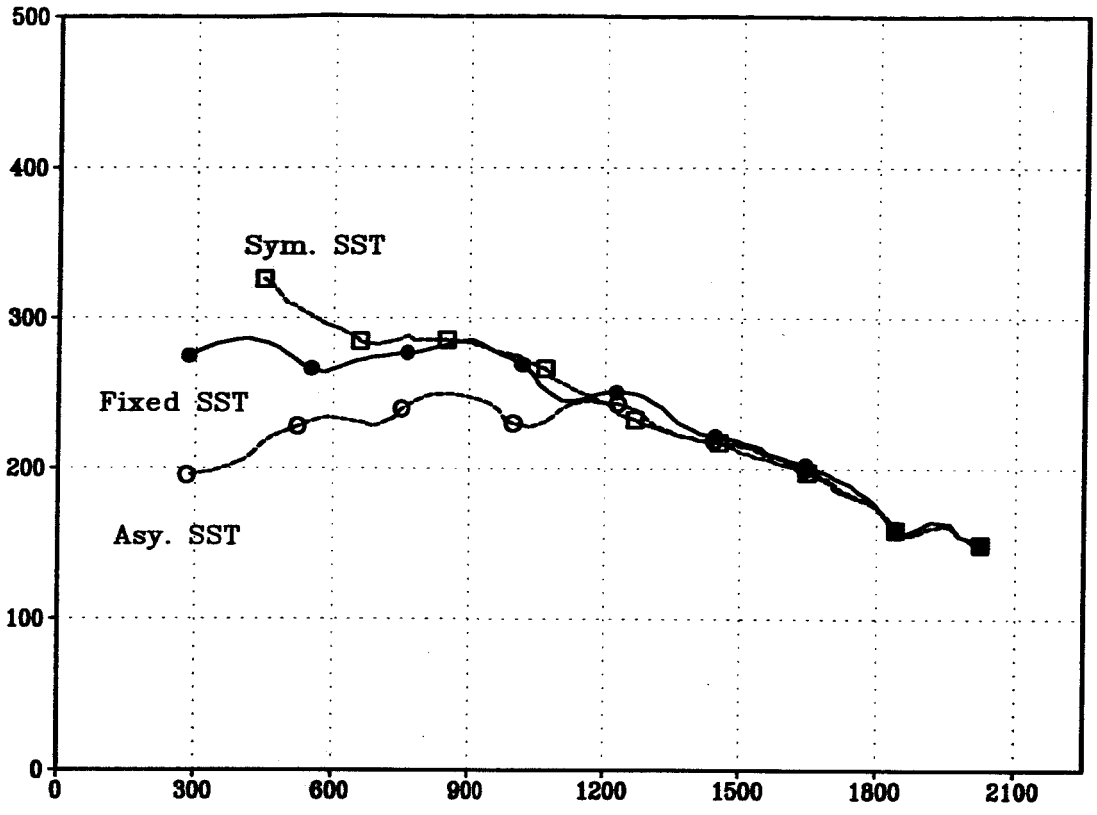

Figure 8: TC tracks in the fixed (solid circles), symmetric (open squares) and asymmetric (open circles) SST experiments.

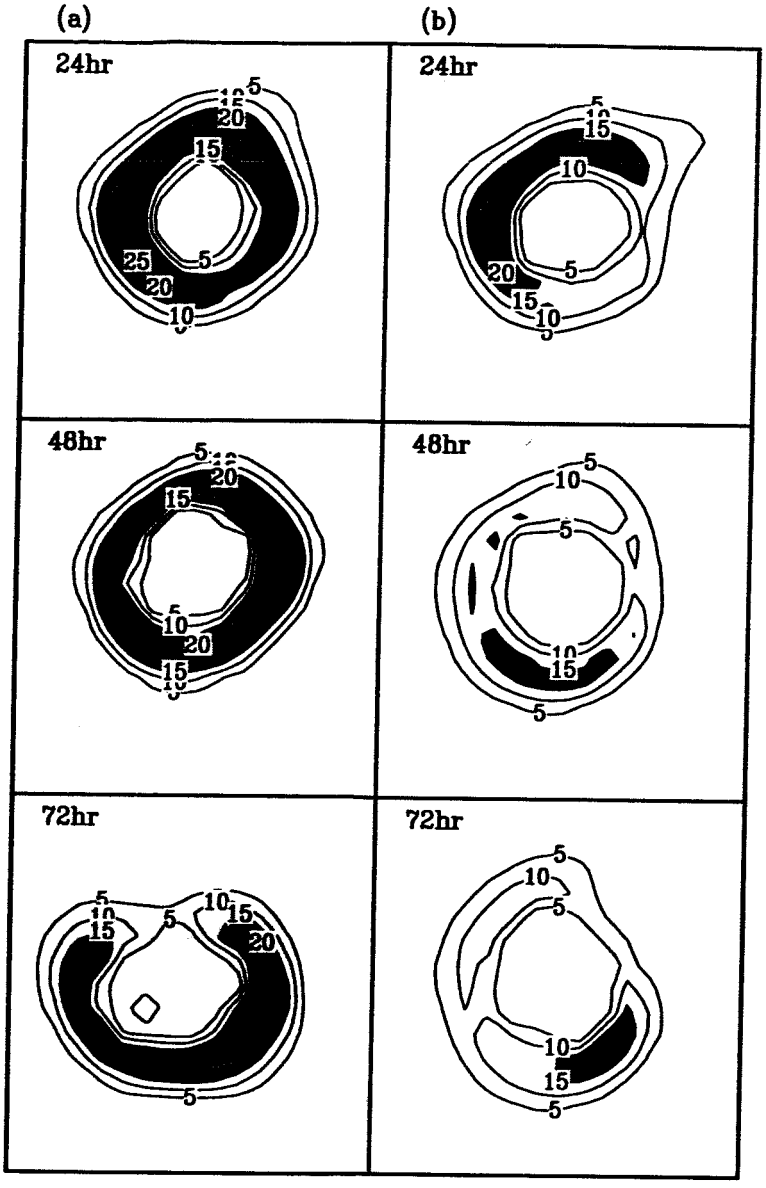

Figure 9: Rainfall rate (mmh^{-1}) in the (a) fixed SST and (b) coupled experiments of E2.

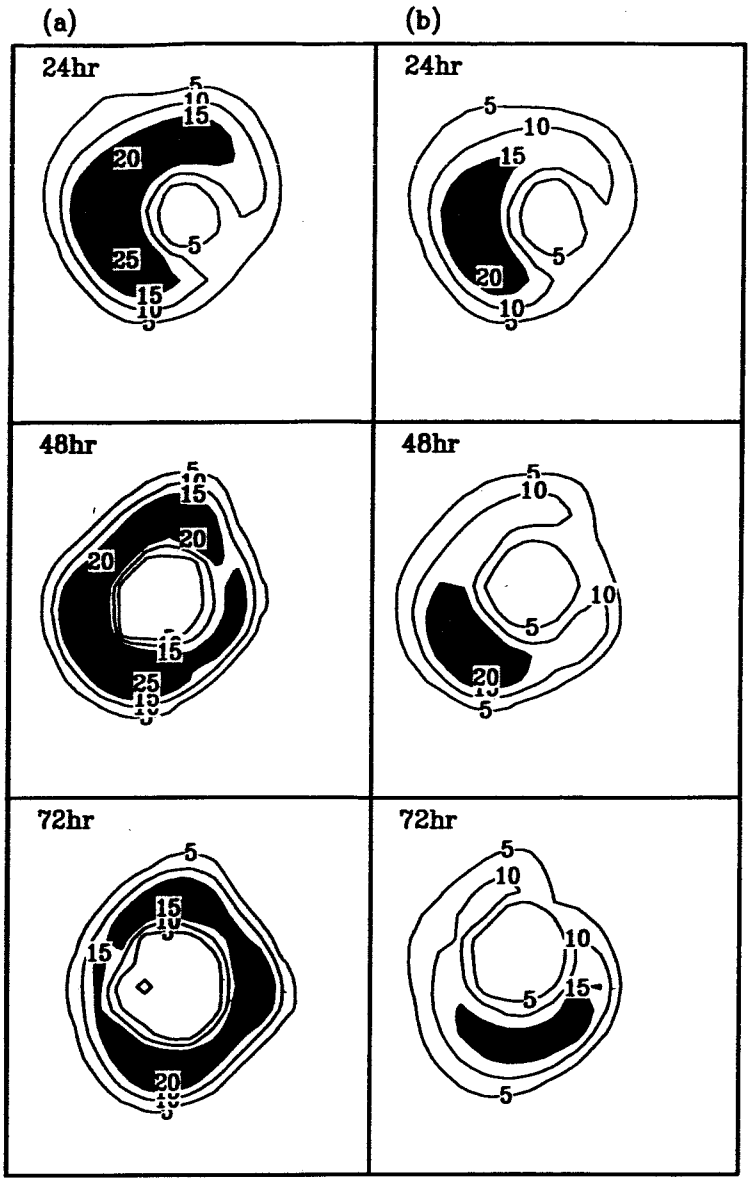

Figure 10: Same as Fig. 10 but for E3.

Impacts of Air-Sea Interaction on Tropical Cyclone Track and Intensity

Liguang Wu[1], Bin Wang[3], and Scott A. Braun[2]

[1]Goddard Earth and Technology Center, University of Maryland at Baltimore County, Baltimore, Maryland

[2]Laboratory for Atmspheres, NASA/GSFC, Greenbelt, Mayland

[3] Department of Meteorology, School of Ocean and Earth Science and Technology, University of Hawaii at Manoa, Honolulu, Hawaii

Summary

A tropical cyclone can generate strong sea surface temperature cooling as it moves over the ocean surface. The resulting cooling can in turn affect tropical cyclone track and intensity. In this study, the influence of hurricane-ocean interaction on tropical cyclone intensity and track is investigated using a coupled hurricane-ocean model. The focus is on how air-sea interaction affects tropical cyclone track and intensity. It is found that the symmetric sea surface temperature cooling with respect to the storm center is primarily responsible for the tropical cyclone weakening in the presence of air-sea interaction. Air-sea interaction has small influence on tropical cyclone track due to the competing processes associated with air-sea interaction. It is also found that the two type track differences simulated in the previous studies likely result from the vortex profiles. By adjusting the vortex outer strength, which is associated with the beta drift, both type of track differences can be achieved.